Measurements of Electron Temperature by Spectroscopy in Hohlraum Targets

C. A. Back, D. H. Kalantar, R. L. Kauffman, R. W. Lee, B. J. MacGowan, D. S. Montgomery, L. V. Powers, T. D. Shepard, G. F. Stone, and L. J. Suter

Lawrence Livermore National Laboratory, P.O. Box 808, Livermore, California 94551

(Received 5 February 1996)

We report on the use of x-ray spectroscopy of mid-Z dopants to measure the electron temperature of hohlraum targets. The hohlraums are gas-filled Au cylinders and, when irradiated with 20 kJ of 0.35 μm laser light, they become mm-sized plasmas bathed in a radiation field. The peak temperatures achieved by the target are 3.7 keV. In addition to being the first electron temperature measurements of the hohlraum itself, these measurements enable an investigation of the thermal energy and electron conduction of the target. [S0031-9007(96)01647-X]

PACS numbers: 52.50.Jm, 52.40.Nk, 52.70.La

Hohlraums have been extensively used as thermal radiation sources because they are reproducible and efficient sources of intense x-ray radiation in the laboratory. Hohlraums are high-Z enclosures, such as cylinders or spheres, that convert high intensity laser energy to an intense x-ray flux [1–4]. In inertial confinement fusion (ICF), one of the two principal approaches in laser-fusion research, they are used to implode capsules. For this reason, past experiments have concentrated on measuring quantities related to the radiative heating, such as the radiation temperature [5–10]. Hohlraums are also used in fundamental studies of opacity, radiation hydrodynamics, and astrophysics [11–13]. The success of their design for specific applications depends on our understanding of their complex environment. To date, few experiments have attempted to experimentally characterize the plasma conditions of the hohlraum itself.

In the Letter we present the first electron temperature measurements of laser-irradiated hohlraums. These measurements are an important advance in hohlraum characterization and are notable in two respects. First, the electron temperature T_e is important because it is one of the few experimental parameters that can be directly compared with complex simulations to help us understand the plasma. In the context of ICF, these measurements can be related to the overall energy balance of the targets. Present ICF targets use gas-filled hohlraums, and for this target design up to 35% of the input laser energy is associated with the underdense plasma formed by ablation of the gas and wall [14]. Experimental measurements such as these are essential to understanding the energy balance and verifying that important unforeseen physical processes are not missing from our numerical simulations of the target. Moreover, T_e is important to evaluate some physical processes such as simulated scattering processes and plasma stagnation which are difficult, if not impossible, to describe analytically.

Second, T_e measurements in hohlraum targets are challenging because of the presence of intense radiation fields. Spectroscopic diagnostics have never been tested in such fields because high radiation temperatures, T_r, are difficult to create in the laboratory. Hohlraums experiments open up a new area of development because their radiation fields are sufficiently intense to actually perturb the atomic kinetics [15] and affect the spectroscopic diagnostics. We choose to use the line ratio of isoelectronic lines from two different elements to diagnose T_e. This technique is advantageous for hohlraum environments because of its relative insensitivity to T_r [16]. These experiments show that this T_e diagnostic is reliable and verifies the temperature to within 10% of the calculated value.

The experiments were performed on the Nova laser using gas-filled hohlraum targets [17]. The hohlraum is a 2.5 mm diameter and 2.5 mm long Au cylinder, with 25 μm thick walls. It is filled to a pressure of 1 atm with neopentane gas, C_5H_{12}. To contain the gas, the laser entrance holes and diagnostic holes used for the spectrometer line-of-sight are covered with thin polyimide membranes that are 6000 Å thick and 1 μm thick, respectively. The dopants are introduced into the hohlraum by a thin CH foil substrate. The foil is a 800 Å thick $\sim$200 μm wide strip of paralyene-n which is coated with a 120 μm wide strip of either 2000 Å of cosputtered TiCr or 3500 Å of KCl. The size of the dopant was chosen to keep the opacity for the spectral lines of interest below one. The foil is stretched over an Au coated C-shaped wire frame having the same radius as the hohlraum and placed in a predrilled slot in the hohlraum Figure 1 shows a schematic of the target as well as an example of the TiCr spectra. Typically the foil was directly irradiated by the beam, though in supplementary shots to study the effects of thermal transport, the foils were not directly irradiated.

Nine of Nova's ten 0.35 μm wavelength laser beams enter the hohlraum through the laser entrance holes of the cylinder to create a pattern of two overlapping rings on the inside surface and provide an intensity of $\sim 3 \times 10^{14}$ W/cm^2 on the hohlraum wall. These hohlraums are larger than the typical hohlraums used in implosion studies due to design criteria discussed in other papers [18]. For these experiments a 1.6 ns laser pulse was temporally shaped and designed to form a

 0031-9007/96/77(21)/4350(4)$10.00

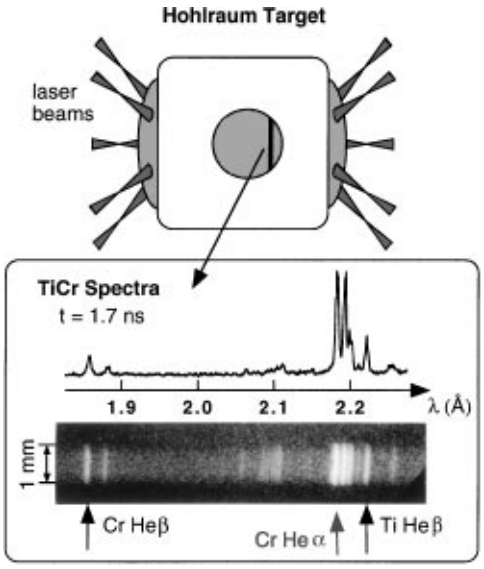

FIG. 1. Hohlraum schematic showing the laser beams and foil position with an example of the data from the gated spectrometer for a TiCr dopant.

long-scale-length plasma with a temperature and density plateau [14]. It starts with a low intensity foot followed by a 800 ps intensity ramp which increases in intensity by a factor of 6.3. During this time, the lasers ablate the CH window and ionize the gas to form a plasma. The ramp is followed by a 600-ps-long intensity plateau during which the laser beams ablate the walls of the hohlraum.

This series of experiments uses the He-like β transition, He β, $1s3p(^1P_1)$-$1s^2(^1S_0)$. K-shell calculations are more reliable than L- or M-shell calculations because the one and two electron K-shell models are inherently simpler and have been validated by many experiments. The beta lines $n = 3$-1 are more useful than the $n = 2$-1 resonance lines as they do not have measurable contributions from underlying satellite lines and their optical depths remain <1 for this experiment, which reduces ambiguities in interpreting the data.

Pairs of dopants were used in these experiments. For temperatures in the 3–5 keV range, Ti and Cr dopants were used because they predominantly ionize to their K-shells at these high temperatures. Furthermore, due to a sufficiently large transition energy (5.6 keV), the TiCr spectra does not overlap with the bright Au M-band background spectra. To cover a lower 1–3 keV temperature regime K and Cl dopants were used. In this case, the Au M band lines are near the dopant K-shell emission, but do not overlap the He-like β lines used for the diagnostic. Note that the useful temperature range of the KCl dopant overlaps that of the TiCr dopants, allowing a cross check of the measurements.

The instruments fielded on the experiment included x-ray spectrometers, x-ray imagers, x-ray streak cameras, and a set of filtered x-ray diodes. The primary diagnostic was an x-ray spectrometer which recorded spectra on gated microchannel plates [19]. The imagers and streak cameras provided time-resolved data of the target x-ray emission from the tracer foils which was important for monitoring the ablation of the target. The x-ray diodes provided a measurement of the radiation field.

The line intensity ratio data from the spectrometers are averaged over the series of shots and are plotted for four times in Fig. 2. Data are corrected for instrument response and the resulting spectra was analyzed using the collisional-radiative code FLY [20]. Error bars on the measurement include the detector uncertainties and the standard error over the series of shots. The timing error was measured to be ± 100 ps. Over these shots the laser energy varied by $\sim 10\%$ and the density variation as measured by the target gas fill pressure was 4%. These translate to insignificant variations for the spectral measurements and are included in the error bars. At early times, the error in the value of the ratio is greater because the signal to noise ratio is smaller and it is asymmetric because the lower bound is limited by detector sensitivity.

The solid line in Fig. 2 is the time-dependent ratio calculated from the plasma parameters predicted by the radiation hydrodynamics simulations using Lasnex [21]. The dash-dotted line and dotted line show the same ratio plotted for $\pm 10\%$ and -30% variations in T_e, respectively. Measurements for times earlier than 0.8 ns are not taken because those spectra are emitted during the ablation phase of the foil when T_e and n_e of the foil are changing. With the exception of data at 1 ns, the measured electron temperatures are within 10% of the values calculated from the simulations. The ratio corresponds to $T_e \geq 3$ keV for the period from 1.2 to 1.7 ns, during which the laser intensity is fairly constant.

The T_e can be inferred from the measured ratios by determining a fit to the data which is self-consistent with

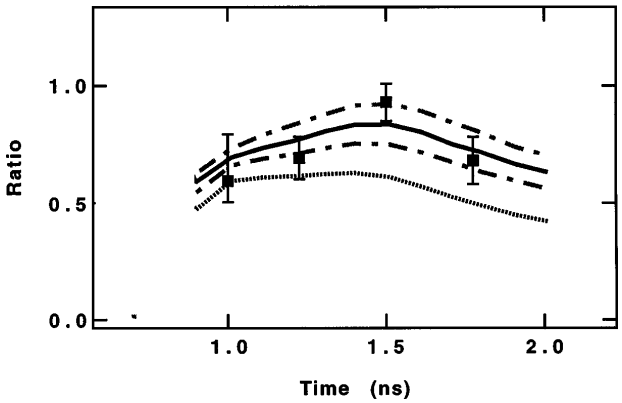

FIG. 2. Line ratio of (CrHeβ/TiHeβ plotted as a function of time. The solid line is the ratio predicted for the calculated hohlraum T_e and n_e histories. The dash-dotted line corresponds to the ratio for a $\pm 10\%$ variation of T_e while the dotted line corresponds to the ratio for a -30% variation of T_e. The squares are the data averaged over several shots.

the measured ratio [22]. Figure 3 shows experimental T_e versus time, along with the laser pulse and the temporal histories of T_e, n_e, and T_r calculated at the position of the tracer dopant. At the beginning, the experimentally determined temperature lags the predictions. The T_e increases to a peak of 3.7 keV at the end of the pulse, then falls after the laser pulse is over. This initial lag compared to calculations may be due to transient effects associated with the beam propagation and heating of the gas. For example, since the laser beams cannot directly illuminate the entire volume of gas inside of the hohlraum, the discrepancy may be related to difficulties in modeling lateral heat flow. More experiments designed to study the initial gas heating are necessary to resolve the details.

Since ablation of the dopant is important, we fielded other diagnostics to simultaneously monitor the density of the dopant. Data from a gated x-ray pinhole camera [23] provided edge-on images of the width of the foil along the hohlraum axis as a function of time. These x-ray images clearly show a stationary foil that ablates 500 ps after the start of the laser pulse. The full-width-half-maximum intensity of the emission, corrected for the initial apparent width of the foil is $250-400$ μm during the last 1 ns of the pulse. Calculations of the foil expansion predict that the width is ~ 250 μm when it has equilibrated with the gas. An estimate of the measured n_e gives electron densities of $(0.8-0.6) \times 10^{21}$ cm^{-3}, clearly showing that the dopant ablates. Once ablated, collisional rates on the order of ps quickly thermalize the dopant with the gas. The T_e diagnostic does weakly depend on n_e. However, even for a worst case assumption of a factor of 2 drop in density, the T_e drops by $<10\%$, thus, with even the lowest estimate of the density, the T_e measurement is not significantly affected.

We also measured the radiation field and experimentally verified that it has a negligible affect on the T_e measurements. Supplementary shots to measure the radiation temperature of the hohlraum, T_r, used a filtered set of absolutely calibrated x-ray diodes, Dante [24]. The data, time, and frequency-dependent fluxes were then input into collisonal-radiative models to quantify the effect of the Au radiation field on the T_e measurements. Calculations show that the measured peak T_r of ~ 180 eV is not large enough to produce perturbations in the ratio and thus does not affect the T_e measurements.

These measurements of T_e allow an investigation of the heating of the hohlraum by two related quantities important to the simulations: the plasma thermal energy and the flux limiter. For a simple model of the plasma, we can estimate the thermal energy from the simple relation $E_{\text{th}} = 1.5 n_e k T_e$ for a gas volume equal to the volume of the hohlraum. This assumes that the underdense plasma is fairly homogeneous in T_e, and measurements of T_e in the hohlraum volume not directly irradiated by a laser beam have supported this assumption. Measurements of the stimulated Brillouin scattered light from these targets show backscattering levels of laser energy $<3\%$ [25], while estimates of stimulated Raman scattered light account for $<6\%$ of the laser energy. Since only $<2\%$ of the laser energy is necessary to completely ionize the gas, the bulk of the laser energy goes into the internal energy of the gas. Figure 4 shows the partition of energy in the target as a function of time, where the squares show the thermal energy as calculated from the measured T_e from the gas. As noted before, this hohlraum target is larger than those typically used to implode capsules, and calculations show that 35% of the energy is expended in heating the underdense plasma. Consequently, the thermal heating of the gas is a significant part of the overall energy absorbed by the target. A comparison shows that the measured thermal energy of the target is fairly consistent with the calculated thermal energy. That we do not measure a large discrepancy indicates that there is no major physical process missing in the large scale simulations of the target.

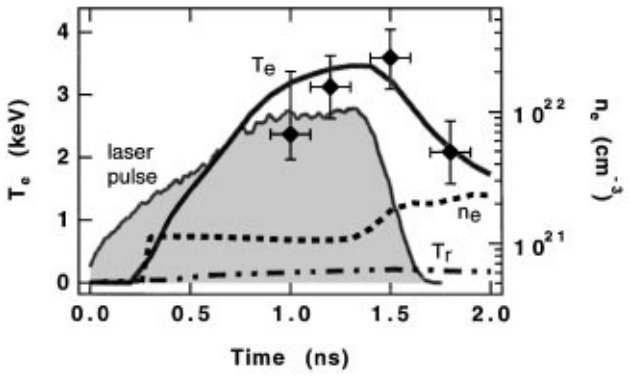

FIG. 3. The electron temperature plotted as a function of time. The measured T_e inferred from the line ratios are shown by the diamonds. Also plotted are the laser pulse shape and calculated T_e, calculated radiation temperature T_r, and calculated electron density n_e.

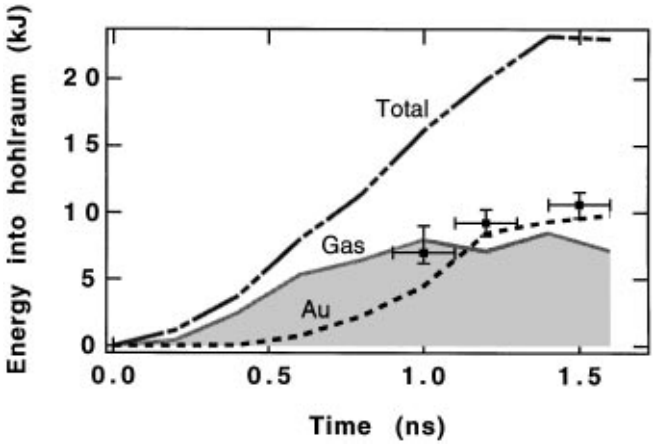

FIG. 4. Energy budget of the target showing the partition of laser energy in heating the target. The squares calculated from the measured T_e compare well with calculated values for the internal energy of the gas.

The dominant physical processes responsible for heating the underdense plasma are inverse bremsstrahlung absorption and electron conduction. Heat flows in calculations of laser-produced plasmas are known to become unphysically large for cases where assumptions for Spitzer heat flow break down. In these cases, a numerical value f is introduced for flux-limited electron conduction. Lasnex simulations at $t = 1.4$ ns show that the experimental T_e is not consistent with extremely low flux limited values such as $f = 0.01$, which produce extremely high temperatures, $T_e = 6.5$ keV. The simulations are also not consistent at the other extreme, $f = 0.5$, where the free-streaming flux models predict low temperatures, $T_e = 2.7$ keV. The range of flux limit values consistent with the error bars of the temperature measurement are 0.025 to 0.150. The typical flux limiter value used for large hohlraums simulations is 0.05 and is derived from open geometry studies of the flux limiters in the corona of laser-produced plasmas. This measured T_e confirms this flux limiter as a reasonable value.

In summary, the measurements, presented here are the first to quantify the electron temperature of the hohlraum itself. Plasma conditions present in hohlraums are a challenge to diagnose because of the high radiation temperatures and the closed-geometry. We show that techniques using tracer plasmas are valid in hohlraums. Measurements of these targets yield $T_e > 3$ keV during the intensity plateau of a shaped laser pulse. The temporal profile of T_e is more peaked than Lasnex calculations, however, the thermal energy contained in the gas is consistent with the partition of energy in hohlraum calculations. These measurements also place bounds on the value of the flux limiter used in these simulations and validate use of a flux limiter of 0.05 for these underdense plasmas. The electron temperature is one of the few measurable quantities that can directly be compared with simulations to test our knowledge of complex closed-geometry plasmas. As such it is a valuable diagnostic that can be applied to future ICF target geometries.

We would like to thank the LLNL target fabrication crew and Luxel Corp. for their creativity and perseverance to develop methods to build these complicated targets. We are also indebted to the Nova crew for their hard work. This work was performed under the auspices of the U.S. Department of Energy by the Lawrence Livermore National Laboratory under Contract No. W-7405-ENG-48.

[1] R. L. Kauffman *et al.,* Phys. Rev. Lett. **73**, 2320 (1994).
[2] R. Sigel, R. Pakula, S. Sakabe, and G. D. Tsakiris, Phys. Rev. A **38**, 5779 (1988); R. Sigel, in *Handbook of Plasma Physics,* edited by A. Rubenchik and S. Witkowski (North-Holland, Amsterdam, 1991), Vol. 3, pp. 163–197, and references therein.
[3] A. Cobble *et al.,* Rev. Sci. Instrum. **66**, 4202 (1995).
[4] H. Nishimura *et al.,* Phys. Rev. A **44**, 8323 (1991).
[5] E. M. Campbell *et al.,* Laser Part. Beams **9**, 209 (1991).
[6] R. Sigel *et al.,* Phys. Rev. Lett. **65**, 587 (1990); N. Kaiser, J. Meyer-ter-Vehn, and R. Sigel, Phys. Fluids **1**, 1747 (1989).
[7] K. Eidemann *et al.,* J. Quant. Spectrosc. Radiat. Transfer **51**, 77 (1994).
[8] L. Suter *et al.,* Phys. Rev. Lett. **73**, 2328 (1994).
[9] A. Hauer, L. Suter, N. Delameter, and D. Ress, Phys. Plasmas **2**, 2488 (1995).
[10] J. L. Porter, T. J. Orzechowski, M. D. Rosen, A. R. Thiessen, L. J. Suter, and J. T. Larsen, Lawrence Livermore Laboratory Report No. UCRL-LR-105820-94, 1994, p. 125.
[11] T. S. Perry *et al.,* Phys. Rev. Lett. **67**, 3784 (1991).
[12] G. Dimonte *et al.,* Phys. Plasmas **3**, 614 (1996).
[13] B. A. Remington *et al.,* Phys. Plasmas **2**, 241 (1995).
[14] L. V. Powers *et al.,* Phys. Plasmas **2**, 2473 (1995).
[15] J. Abdallah *et al.,* J. Quant. Spectrosc. Radiat. Transf. **50**, 91 (1993).
[16] S. Marjoribanks, M. C. Richardson, P. A. Jaanimagi, and R. Epstein, Phys. Rev. A **46**, R1747 (1992); T. S. Shepard *et al.,* Lawrence Livermore Laboratory Report No. UCRL-LR-105820-94, 1994, p. 137.
[17] G. Stone, Lawrence Livermore Laboratory Report No. UCRL-MA-119389, 1995.
[18] V. Powers *et al.,* Phys. Rev. Lett. **74**, 2957 (1995).
[19] C. A. Back *et al.,* Rev. Sci. Instrum. **66**, 764 (1995).
[20] R. W. Lee and J. T. Larsen, (to be published); R. W. Lee, B. L. Whitten, and R. E. Strout, J. Quant. Spectrosc. Radiat. Transfer **32**, 91 (1984).
[21] G. Zimmerman and W. Kruer, Comments Plasma Phys. Control. Fusion **2**, 85 (1975).
[22] C. A. Back *et al.,* "Spectroscopic Temperature Measurements in Nonequilibrium Plasmas," in Proceedings of the 10th Topical Conference on Atomic Processes in Plasmas, 1996 (AIP, New York, to be published).
[23] O. L. Landen *et al.,* Proc. SPIE Int. Soc. Opt. Eng. **2002**, 2 (1993).
[24] H. N. Kornblum, R. L. Kauffman, and J. A. Smith, Rev. Sci. Instrum. **57**, 2179 (1986).
[25] R. E. Turner *et al.,* Lawrence Livermore Laboratory Report No. UCRL-LR-105821-95-2, 1995, p. 97.